Roughening transition on Cu(113): A quantitative analysis of new experimental results

B. Salanon, F. Fabre, and J. Lapujoulade
Service de Physique des Atomes et des Surfaces (DPhG/PAS), Département de Physique Générale, Institut de Recherche Fondamentale, Centre d'Etudes Nucléaires de Saclay, 91191 Gif-sur-Yvette Cédex, France

W. Selke
Institut für Festkörperphysik der Kernforschungsanlage Jülich, D-5170 Jülich, Federal Republic of Germany
(Received 11 January 1988)

From an analysis of the peak shapes in helium-diffraction experiments on Cu(113), the roughening transition temperature is estimated to be 720±50 K. From fits to the experimental results of Monte Carlo data on various models, particularly on a terrace-step-kink model, effective energies for the creation of a kink on a step, W_0, and for the interaction between steps, W_n, are obtained as $W_0=800\pm50$ K and $W_n=560\pm50$ K.

I. INTRODUCTION

Roughening phenomena have been studied in much detail since the first theoretical work by Burton, Cabrera, and Frank,[1] which showed that crystal faces are flat at low temperatures, but may become rough at and above the roughening transition temperature T_R.[2] In particular, the nature of that transition is very subtle and it is usually described by a Kosterlitz-Thouless–type theory.[3] On the experimental side, thermal roughening has been observed, for instance, directly for solid-helium crystal shapes,[4] and convincing indirect evidence for roughening has been provided for various other materials as well.[2]

As far as close-packed faces of metals are concerned, it was believed for a long time that possible roughening transition temperatures would be higher than bulk melting temperatures. Only a few years ago Lapujoulade *et al.*[5] suggested—on the basis of helium-diffraction experiments—that stepped (11l), l-odd, faces of copper may undergo roughening transitions well below the melting point. Subsequent theoretical interpretations were given by Villain, Grempel, and Lapujoulade[6] (hereafter abbreviated as VGL) for copper and by den Nijs *et al.*[7] for helium-diffraction experiments on Ni(115), providing additional evidence for roughening transitions. However a fully quantitative and generally accepted theoretical analysis of these and other recent experimental findings on both copper[8] and nickel[9] is still missing. Specifically, the VGL approach describes the (11l) faces as (100) terraces separated by steps with effective energies to create a kink on a step and to shift a step with respect to the neighboring ones. This is[6] in contrast to a description based on nearest-neighbor bond energies which does not explicitly include step-step interactions.[7,9]

The VGL picture has been applied to the case of the (113) face of copper in a Monte Carlo (MC) study of Selke and Szpilka[10] for a simplified terrace-step-kink (TSK) model characterized by two parameters for the effective kink creation energy W_0 and the step-step interaction energy W_n. In particular, they showed that the measured helium-diffraction intensities[5,6] could be reproduced quite well, assuming a roughening transition temperature T_R of about 650±50 K.[10] This estimate turned out to be largely independent of the actual ratio W_n/W_0 with a typical onset of the sharp decrease in intensity occurring at roughly $0.8T_R$, a behavior reminiscent of that for other quantities close to the roughening temperature.[2]

In this article we report on new helium-diffraction measurements of peak shapes for Cu(113) and their quantitative interpretation in terms of various microscopic models, especially the TKS model studied by Selke and Szpilka. The analysis of peak shapes allows us to estimate T_R as well as the effective energies W_0 and W_n.

The outline of the paper is as follows: In Sec. II some of the main ideas of the VGL approach are briefly recalled and various models intended to mimic the (113) face are introduced. In Sec. III we present fits of the experimental results to Monte Carlo data for the TSK model and an anisotropic discrete Gaussian model[2] as well as to analytic expressions for an anisotropic body-centered solid-on-solid (BCSOS) model.[11] Estimates for T_R, W_0, and W_n are given and we discuss the thermal behavior of the kink density. A short summary concludes the article.

II. ANALYSIS OF VARIOUS MODELS

A. Roughening of the (113) face

The perfect (113) face consists of (100) terraces separated by (111) steps. Its structure is depicted in Fig. 1 together with that of Cu(110), whose terraces and steps have (111) orientation; similarities between the two structures will be used below.

Thermal excitations cause the steps to meander by forming kinks. Eventually a roughening transition will occur at the roughening temperature T_R. The disorder induced by the meandering steps may be described by the fluctuations of the step positions (or by the fluctuations of the surface height relative to a reference plane), i.e., by the correlation function $G(r)=\langle[h(r)-h(0)]^2\rangle$, where $h(r)$ is the step function displacement (or height) at point

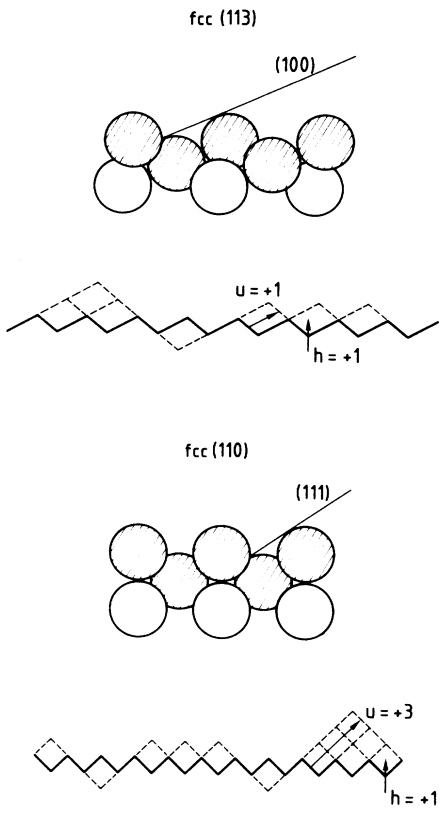

FIG. 1. Schematic representation of the fcc (110) and fcc (113) faces showing their similarities. The disordered structures are denoted either by the step displacement u or the height h normal to the face.

r, r being a two-dimensional vector. In the case of a Kosterlitz-Thouless–type roughening transition, in the limit of divergent distance ($|r| \to \infty$) $G(r)$ approaches a finite value for temperatures below T_R, while it diverges logarithmically in that limit for $T \geq T_R$. The microscopic behavior is related to the macroscopic shape of crystals through the surface tension. Around a specific orientation of the crystal face, sharp facets exist only for $T < T_R$, whereas the crystal is rounded for $T > T_R$.[2,3] Helium-diffraction experiments provide microscopic information on the surface topography over distances of typically 10–100 Å.

To interpret helium-diffraction data on Cu and Ni (11l) faces, two types of models have been considered. Villain *et al.* introduced Hamiltonians describing the energetics of the faces in terms of effective kink-creation and step-step interaction energies.[6] den Nijs *et al.* proposed a model which does not include explicitly the step-step interaction, but only nearest-neighbor interactions.[7] (It causes the difference between the two approaches to become more pronounced as l increases). In the latter case a scaling relation for T_R as a function of l is obtained. As shown below, our experimental results support neither this scaling relation nor the type of anisotropy of $G(r)$ suggested by den Nijs *et al.*, but they can be explained quantitatively quite well within the VGL approach.

In the following subsections some of the main aspects of the VGL approach are recalled. This approach is then applied in the analysis of various models exhibiting the salient features of the roughening of the (113) face.

B. The VGL approach (Ref. 6)

The VGL approach[6] may be applied to a variety of microscopic models for roughening transitions, particularly on (11l) faces. The surface energy is expressed in terms of a continuous variable for the step displacement (or surface height) in a sine-Gordon–type form, i.e., the free energy is that of an anisotropic harmonic lattice adding a localization term to favor integral values of the displacement. Explicitly, the free energy is written as

$$\mathcal{F}=\tfrac{1}{2}\sum_{q}(\eta q_n^2+\eta' q_m^2)\,|\,u_q\,|^2+V\sum_{m,n}[1-\cos(2\pi\tilde{u}_{m,n})]\ . \tag{1}$$

$u_{m,n}$ is the step-displacement variable for step m at position n; u_q is its Fourier transform. The variable $\tilde{u}_{m,n}$ that appears in the cosine (or localization) term is the long-wavelength part of $u_{m,n}$. The surface tensions η and η' refer to the directions parallel and perpendicular to the steps, respectively; they depend on temperature. A renormalization analysis[6] shows that the localization potential V vanishes above T_R and that the free energy becomes purely harmonic. Then, from the equipartition theorem for the normal modes u_q, the correlation function $G(r)=G(m,n)$ is obtained as

$$G(m,n)=\Gamma(\rho)=\frac{T}{\pi(\eta\eta')^{1/2}}\ln\rho+\text{const} \tag{2}$$

with

$$\rho^2=m^2\left[\frac{\eta}{\eta'}\right]^{1/2}+n^2\left[\frac{\eta'}{\eta}\right]^{1/2}\ .$$

For $T<T_R$, $G(m,n)$ remains bounded even for large values of m and n. The roughening transition temperature T_R is determined by the following identity:

$$\frac{T_R}{[\eta(T_R)\eta'(T_R)]^{1/2}}=\frac{2}{\pi}\ , \tag{3}$$

where η and η' are the renormalized surface tensions.

Under the assumption that the surface is made of domains of constant height and that diffraction from domain walls is negligible, the scattered intensity can be written as

$$I(\Delta\mathbf{K})=I_0(\Delta\mathbf{K})\sum_{m,n}e^{i\,\Delta\mathbf{K}\cdot\mathbf{R}_{nn}}\langle e^{i\,\Delta\mathbf{k}\cdot\mathbf{t}(u_{mn}-u_{00})}\rangle\ . \tag{4}$$

$\Delta\mathbf{K}$ is the momentum transfer parallel to the face, $\Delta\mathbf{k}$ is the total momentum transfer, and $\mathbf{t}$ is the elementary translation between domains. $I_0(\Delta\mathbf{K})$ is the form factor of the ordered face. Using a Gaussian approximation for the thermal averages, Eq. (4) can be transformed into

$$I(\Delta\mathbf{K})=I_0(\Delta\mathbf{K})\sum_{\mu,\nu}\frac{\Gamma(2-\tau)}{\Gamma(\tau/2)\Gamma((3-\tau)/2)}\left[\left[\frac{\eta}{\eta'}\right]^{1/2}(a_y\,\Delta K_y+2\pi\mu)^2+\left[\frac{\eta'}{\eta}\right]^{1/2}(a_x\,\Delta K_x+2\pi\nu)^2\right]-\left[1-\frac{\tau}{2}\right], \quad (5)$$

i.e., a superposition of power laws centered at Bragg positions, ν,μ being the peak indices. ΔK_x and ΔK_y are the components of $\Delta\mathbf{K}$, respectively, perpendicular and parallel to the steps. a_x is the distance between adjacent steps and a_y is the interatomic distance along steps. τ is given by

$$\tau=\frac{T\pi}{4(\eta\eta')^{1/2}}[1-\cos(\Delta\mathbf{k})\cdot\mathbf{t})] . \quad (6)$$

When the incidence conditions are varied, τ varies between zero and a maximum, $\tau_{\max}$. $\tau=0$ corresponds to in-phase conditions where interferences from different domains are constructive, giving rise to a Bragg peak. $\tau=\tau_{\max}$ corresponds to antiphase conditions, for which the peak of interest is broadened and exhibits a high sensitivity to surface disorder. By fitting the experimentally observed peak shapes, preferably under antiphase conditions, estimates for τ and η/η' can be obtained. Therefore, from helium-diffraction experiments on stepped faces undergoing a roughening transition, quantities such as the anisotropic surface tensions can be determined.

C. A terrace-step-kink model

In a previous study on Cu(113), Selke and Szpilka considered the following Hamiltonian:[10]

$$\mathcal{H}=\sum_{m,n}W_0(u_{m,n+1}-u_{m,n})^2+\sum_{m,n}f(u_{m+1,n}-u_{m,n}) . \quad (7)$$

W_0 is an effective kink-creation energy describing the interactions along steps; f is an effective interaction between steps (averaging over near-neighbor bond energies as well as long-range elastic and dipolar forces) and is given by

$$f(\Delta u)=\begin{cases}0 \text{ for } \Delta u\geq 0 ,\\ W_n \text{ for } \Delta u=-1 ,\\ \infty \text{ for } \Delta u<-1 .\end{cases}$$

W_n is the effective energy per atom to shift steps towards each other from their crystallographic. Overhangs or double steps are forbidden by the condition for $\Delta u<-1$. It is assumed that no energy is needed to move steps apart from each other from their crystallographic positions, reflecting the rapid decrease of the forces between steps (of elastic or dipolar origin). Of course, the model involves some drastic simplifications. However, as has been shown earlier[6,10] and as will be shown below, the model seems to contain the essential physics to describe roughening phenomena on stepped faces. It should be noted that in the ansatz of an effective step-step interaction parameter W_n, the details of the crystallographic structure can be presumably neglected. In particular, we do not take into account that the atoms in adjacent steps are shifted relative to each other by one-half an interatomic distance.

To determine from the model the experimentally relevant quantities τ and η/η' [see Eqs. (4) and (5)] as functions of temperature, we calculated the correlation function $G(m,n)$ using Monte Carlo techniques. In agreement with the VGL approach, $G(m,n)$ is well described by Eq. (2), even for relatively small values of m and n, and therefore estimates for η and η' can be obtained quite easily from best fits of the Monte Carlo data. The roughening transition temperature follows from the universality relation (3).

We performed standard Monte Carlo simulations on systems of M steps with M atoms along each step. Full periodic boundary conditions were used. Usually we chose $M=50$; a few runs were done with $M=100$ to check possible size dependencies of the estimates for η and η' (no appreciable finite-size effect was detected). We considered three different values of the ratio W_n/W_0, namely $W_n/W_0=1$, 0.2, and 0.7. In the case of weak interactions between steps, typical relaxation and fluctuation times become quite large and run lengths of at least a few 10^5 Monte Carlo steps per site (MCS/S) were necessary to obtain reliable results.

Typical results for $G(m,n)$ are displayed in Fig. 2, showing the correlations parallel and perpendicular to the steps at a temperature above T_R. Obviously the ex-

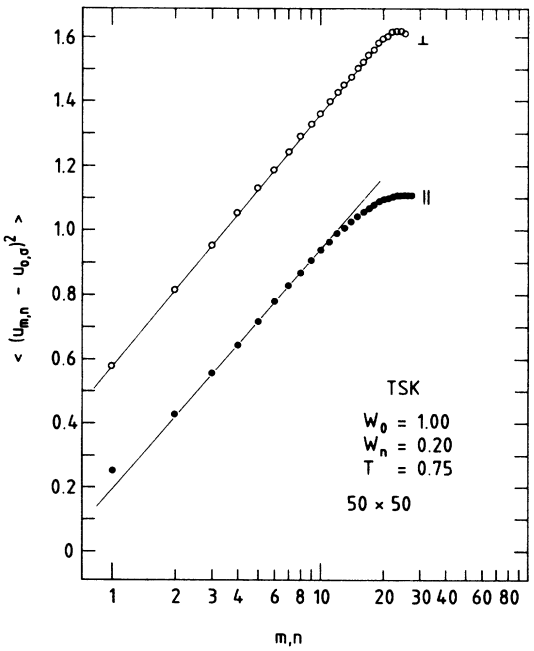

FIG. 2. Typical correlation function for the TSK model, $W_0=1.00$, $W_n=0.20$, $T=0.75$, sample size 50×50, and length of Monte Carlo run 4×10^5 MCS/S.

pected logarithmic behavior already holds for quite short distances. The rounding at distances close to one-half of the linear dimension of the system, i.e., $M/2=25$, is mainly due to the periodic boundary conditions. These and similar results confirm that the roughening transition is, indeed, of Kosterlitz-Thouless type for the TSK model (also see Refs. 6 and 10) with the prefactor in front of the logarithmic term taking a universal value at T_R. The estimates obtained for τ and η/η' are discussed in Sec. II E together with results on variants of the model.

D. The anisotropic BCSOS model

Although Monte Carlo methods are very powerful and versatile, it is convenient to have analytical expressions at one's disposal, especially when fits to the experiment are needed.

Villain *et al.* studied the case of a very large anisotropy ($W_n \ll W_0$); neglecting the renormalization of η' (i.e., setting $\eta'=W_n$), they calculated the value of η in a one-dimensional approximation for a single step. They found $\eta=(T/2)e^{W_0/T}$. Nevertheless, in spite of their qualitatively correct behavior, the above formulas suffer from various uncertainties which preclude precise determination of W_0 and W_n. It is shown below that exact analytical results may be obtained for the anisotropic body-centered solid-on-solid (BCSOS) model,[11] which turns out to be closely related to the TSK model.[10]

As discussed above, the TSK model introduces effective couplings between neighboring steps, disregarding some aspects of the geometry (shift of one-half an interatomic distance in the atomic position in adjacent steps). Indeed, by studying in the following the anisotropic BCSOS model,[11] we show that the details of the geometry are of minor importance, once the values of the kink-creation energy W_0 and of the effective interaction between adjacent steps, W_n, have been fixed.

The anisotropic BCSOS model[11] describes the roughening of the (110) face of a fcc crystal. Possible configurations are depicted in Fig. 3, together with those of the TSK model and the real (113) face, exhibiting the differences in the details of the geometry. We now introduce anisotropic couplings J_x and J_y, which may be interpreted in the same spirit as the effective couplings in the TSK model, i.e., J_x corresponds to the kink-creation energy, while J_x denotes the effective interaction between adjacent steps. In spite of the different geometry [see Figs. 3(a)–3(d)], it follows immediately that the simplest excitations with only one kink cost the same energy for the TSK model and the anisotropic BCSOS model, provided $J_y=W_0$ and $2J_x=W_n$. Using these identities, we found good agreement between analytical results on the BCSOS model and the numerical data for the TSK model, demonstrating that geometrical aspects are of rather minor relevance.

Similar to the isotropic case,[11] exact results on the anisotropic BCSOS model may be obtained via the correspondence to six-vertex models.[12,13] The roughening transition is of the Kosterlitz-Thouless type. The transition temperature T_R is given by

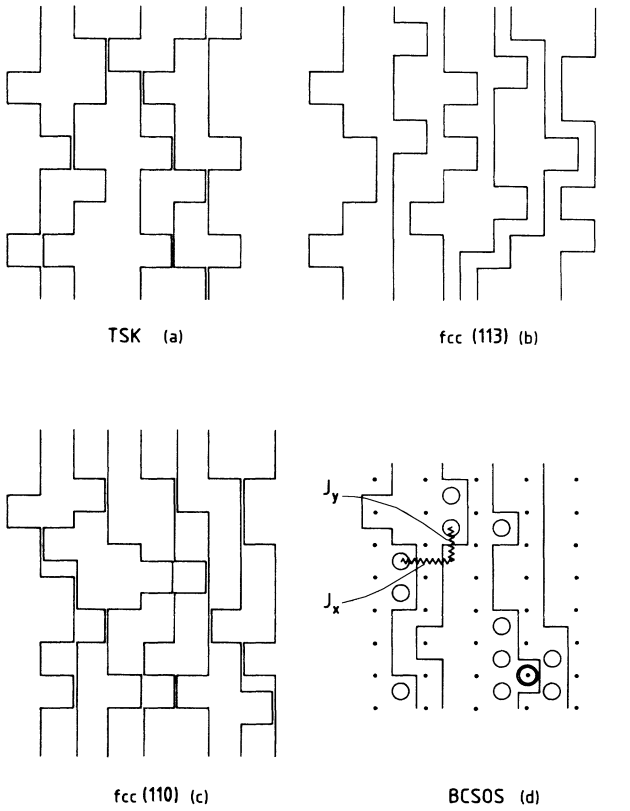

FIG. 3. Step configurations for (a) the TSK model, (b) a fcc (113) face, and (c) a fcc (110) face. Panel (d) shows the correspondence between step positions and atomic heights in relation with the BCSOS model. ● represents atoms in layer 1, ○ atoms in layer 2 (above 1), and atoms in layer 3. J_x and J_y are the coupling constants referred to in the model.

$$\Delta(T_R)=-1 , \tag{8}$$

where

$$\Delta(T)=(x^2+y^2-1)/2xy , \tag{9}$$

with $x=\exp(-J_x/k_BT)$ and $y=\exp(-J_y/k_BT)$. For $T\geq T_R$ and for large distances, the correlation function $G(m,n)$ can be written as

$$G(m,n)=\langle(u_{m,n}-u_{0,0})^2\rangle=A(T)\ln\rho+\text{const} , \tag{10}$$

with $\rho^2=m^2+\lambda^2n^2$ and

$$A(T)=(2/\pi^2)[\tfrac{1}{2}-(1/\pi)\arcsin\Delta(T)]^{-1} . \tag{11}$$

A comparison to the VGL approach (see Sec. II B) yields

$$(\eta\eta')^{1/2}=(\pi/2)T[\tfrac{1}{2}-(1/\pi)\arcsin\Delta] . \tag{12}$$

The anisotropy λ^2 ($=\eta/\eta'$; see Sec. II B) is known exactly only for $T=2T_R$, where

$$\lambda^2=\eta/\eta'=x^2/y^2 . \tag{13}$$

As will be argued below, Eq. (13) seems to give a good ap-

proximation also at other temperatures $T \geq T_R$. It should be noted that for the BCSOS model the surface roughness is limited due to the constraint that the height differences at neighboring sites cannot be larger than unity. One obtains $A(T \to \infty) = 6/\pi^2$, and the exponent $\tau/2$ in the power law describing the line shape of the diffraction peaks [Eq. (4)] has a maximal value of $\frac{3}{2}$.

Expanding $\tau/2$ for T close to T_R leads to

$$\tau/2 = \tfrac{1}{2} + C(T - T_R)^{1/2} , \tag{14}$$

i.e., τ is expected to exhibit a cusp at T_R. The question of its observability is discussed in Sec. III.

E. The anisotropic discrete Gaussian model

To clarify the role of details of the models on the estimates for the experimentally relevant parameters η and η', we also studied the anisotropic discrete Gaussian (DG) model. In this model the step-step interaction [compare to Eqs. (6) and (7)] is described by a harmonic term as the kink-creation energy, but with a different prefactor. Explicitly, the Hamiltonian can be written in the form

$$\mathcal{H} = \sum_{m,n} J_x (u_{m+1,n} - u_{m,n})^2 + J_y (u_{m,n+1} - u_{m,n})^2 . \tag{15}$$

Comparison of the energies for the lowest excitations, such as single kinks, with those in the TSK model yields the correspondence $J_y = W_0$ and $2J_x = W_n$ (restriction to low-lying excitations seems to be reasonable, because, even at the roughening temperature, mainly these excitations do occur).

At high temperatures the corresponding values of η and η' can be easily determined:[14]

$$\eta = 2J_y \quad \text{and} \quad \eta' = 2J_x . \tag{16}$$

So the correlation function follows as

$$G(m,n) = \frac{T}{4\pi (J_x J_y)^{1/2}} \times \ln \left[m^2 \left[\frac{J_y}{J_x} \right]^{1/2} + n^2 \left[\frac{J_x}{J_y} \right]^{1/2} \right] . \tag{17}$$

Accordingly, the exponent τ is linear at high temperatures. In the experimentally interesting antiphase condition,[5] one then has

$$\frac{\tau}{2} = \frac{\pi}{8} \frac{T}{(J_x J_y)^{1/2}} . \tag{18}$$

Using the universality relation [see Eq. (3)], which is expected to hold for transitions of the Kosterlitz-Thouless type, and extrapolating the high-temperature results to lower temperatures, one obtains the rough estimate

$$k_B T_R \simeq (4/\pi)(J_x J_y)^{1/2} , \tag{19}$$

which may be compared, for instance, in the isotropic case ($k_B T_R / J \sim 1.28$), to the supposedly accurate estimate based on extensive Monte Carlo work [$k_B T_R / J \simeq 1.45$–1.48 (Ref. 15)]. Therefore a simple extrapolation of the analytical high-temperature results is somewhat questionable, and we performed Monte Carlo simulations on the anisotropic DG model to determine the temperature dependence of η and η' for various anisotropies. Again, runs of length of about 10^5 MCS/S were

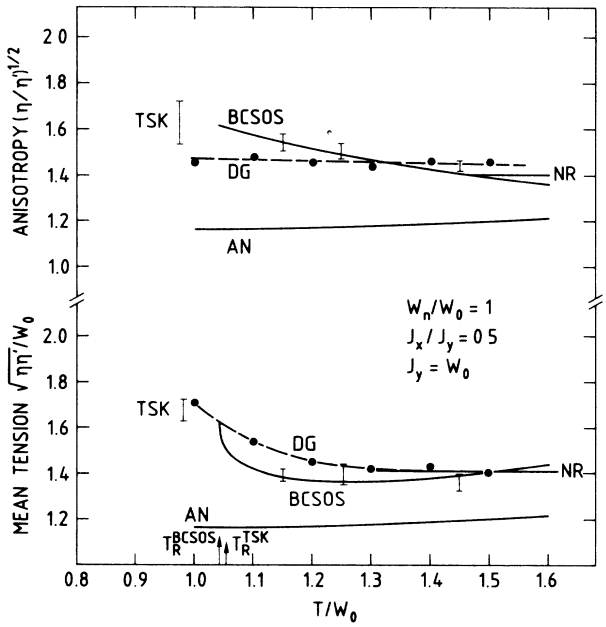

FIG. 4. Comparison between the anisotropy η/η', and the mean surface tension $[(\eta\eta')^{1/2}]$ for various models. Error bars are Monte Carlo results for the TSK model, $\times$ are Monte Carlo results for the discrete Gaussian model (DG) (dashed line is a guide for the eye), AN (solid line) corresponds to $\eta = W_n$, $\eta' = (T/2)e^{W_0/T}$ of VGL, and NR is the unrenormalized result. $W_n/W_0 = 1$ for TSK and $J_x/J_y = 0.5$ for BCSOS ($J_y = W_0$).

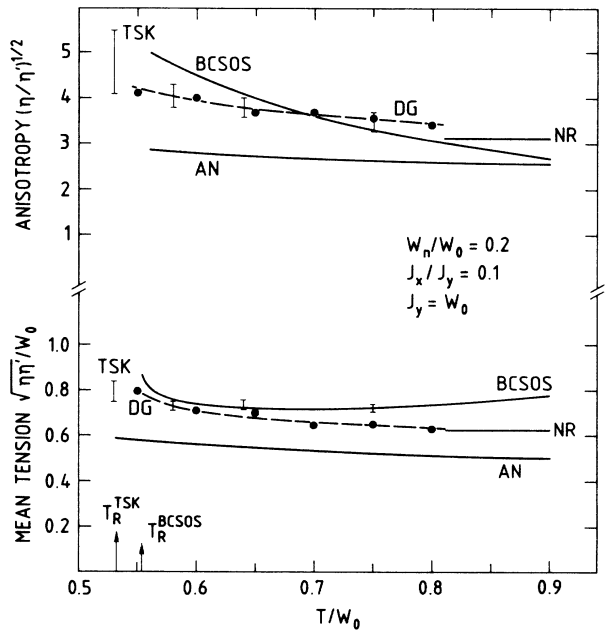

FIG. 5. Same as Fig. 4, but with $W_n/W_0 = 0.20$, $J_x/J_y = 0.10$.

done using a vectorized algorithm suitable for a Cray computer.

Results of the various models will be discussed and compared in the following subsection.

F. Comparison of results on the various models

As described in Sec. II C, estimates for η and η' can be obtained by fitting Monte Carlo data on the correlation function $G(m,n)$ to the ansatz given in Eq. (2). Using the approximate transcriptions relating (W_0, W_n) to (J_x, J_y), one may then compare these estimates for the TSK and anisotropic DG models with each other and with the analytical expressions for the anisotropic BCSOS model [see Eqs. (12) and (13)].

Results on the anisotropy η/η' and the mean surface tension $[\simeq(\eta\eta')^{1/2}]$ for W_n/W_0 (or $2J_x/J_y)=1$ and 0.2 depicted in Figs. 4 and 5. We also included the approximate formulas of VGL (denoted by AN) (expected to hold only for $W_n \ll W_0$; see Sec. II D) and, for the discrete Gaussian model, its high-temperature "nonrenormalized" (NR) values. In the case of the anisotropic BCSOS model the anisotropy η/η' may be approximated by Eq. (13) at temperatures different from $2T_R$ (which is justified *a posteriori*).

Obviously the results for the anisotropic DG and the TSK models are quite similar at temperatures in between T_R and about $2T_R$, reflecting that only a few double (or triple) kinks are present at these temperatures. Also, the results on the anisotropic BCSOS model do not differ greatly, which shows that geometrical details do not play a significant role. The increase of the mean surface tension $(\eta\eta')^{1/2}$ at high temperatures is due to the constraint on the height differences preventing large disorder. In the case of the DG model the high-temperature limiting values are approached rather rapidly. The approximate formulas of VGL seem to underestimate both the anisotropy and the surface tension appreciably upon lowering the temperature towards T_R.

At any rate, for the ratios we considered we can conclude that slight differences between the DG, TSK, and BCSOS models are apparent, but, nevertheless, the resulting values for $\eta=\eta(T)$ and $\eta'=\eta'(T)$ are rather insensitive to the details of the Hamiltonians. This suggests that the kink-creation energy W_0 and the step-step interaction energy W_n may be estimated unambiguously and rather precisely by comparison of the data on the models to experimental results.

III. EXPERIMENT AND ANALYSIS

The experimental apparatus has been fully described elsewhere.[16] The Campargue-type nozzle beam was operated at two energies (21 and 63 meV). Most experiments were performed with the incidence plane perpendicular to close-packed rows. The detector could be rotated in and out of the incidence plane so that the shape of the specular peak could be measured in two orthogonal directions.

The sample was cut from a copper single crystal; after desulfurization it was mechanically and electrochemically polished. Is was then cleaned *in situ* by cycles of argon-ion bombardment (400 V, 10 μA, 1 h) and annealing at 800 K. Such a treatment was pursued until diffracted intensities were steady. Figure 6 shows the measurements of the specular-beam width [full width at half maximum (FMHM)] versus the incidence angle θ_i. For a sample temperature of 70 K only a slight oscillation of the width is visible, reflecting the presence of a small amount of disorder. Moreover, the minimal width, corresponding to in-plane conditions, is $\Delta\theta=0.70°$, while a direct measurement of the incident beam yields $\Delta\theta=0.55°$.

The residual disorder brought about by various crystal imperfections is thus low. For $T=770$ K the specular width exhibits very strong oscillations. The location of extrema corresponds to phase and antiphase conditions between domains, except for a small shift that can be ascribed to an outward relaxation. Such a behavior clearly shows that the Cu(113) face becomes rough through the formation of kinks along steps. Peak profiles were measured as functions of the crystal temperature. In our analysis the influence of inelastic scattering was taken into account by the following procedure. Figure 7 shows the specular peak for increasing crystal temperatures. For in-phase conditions it is clear that the peak width at half maximum is constant, whereas the inelastic background steadily increases. It is easy to fit such profiles by the sum of a Gaussian of constant width and of a Lorentzian function meant to represent the background. For each temperature such a Lorentzian was determined and subtracted from the antiphase profile, as inelastic

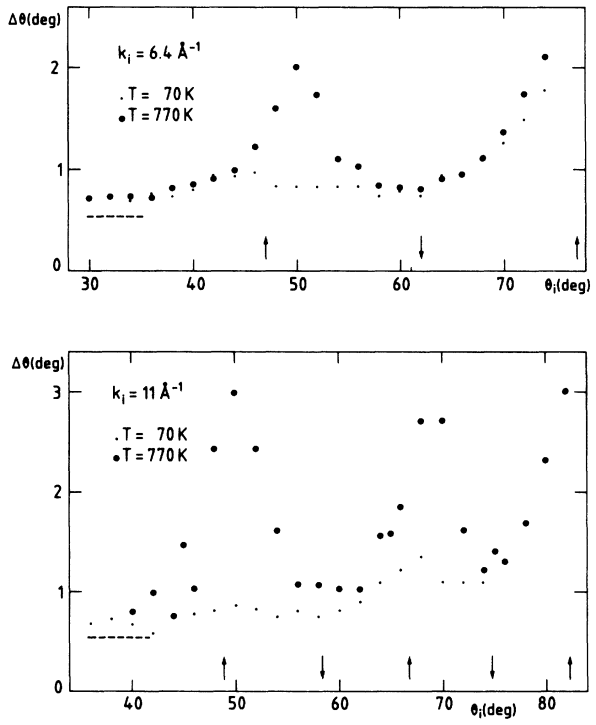

FIG. 6. Variation of the angular width $\Delta\theta$ (FWHM) of the specular peak. The horizontal dotted line represents instrumental width ($k_i=6.4$ and 11 Å^{-1}).

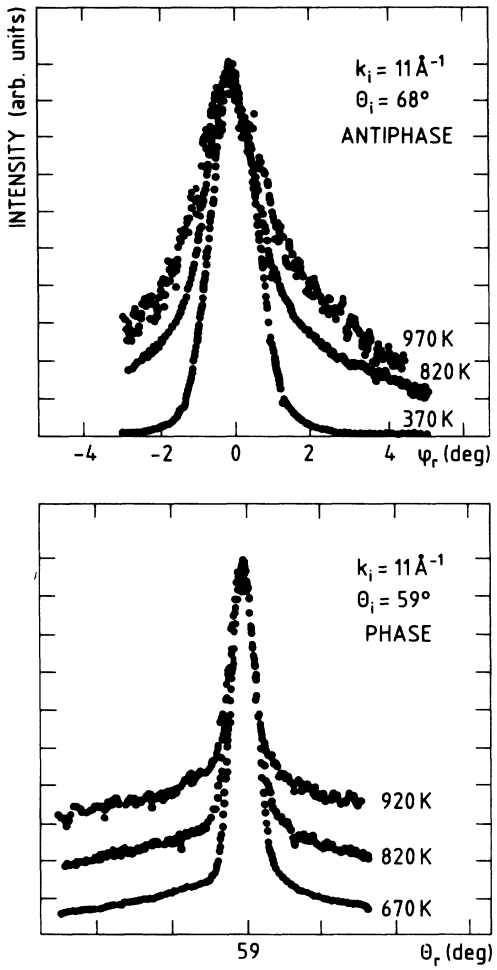

FIG. 7. Cu(113)/He. Intensity profiles for the specular peak under antiphase conditions (top) and in-phase conditions (bottom). The incidence plane is normal to the steps; measurements were made in (θ_r) and out (φ_r) of the incidence plane.

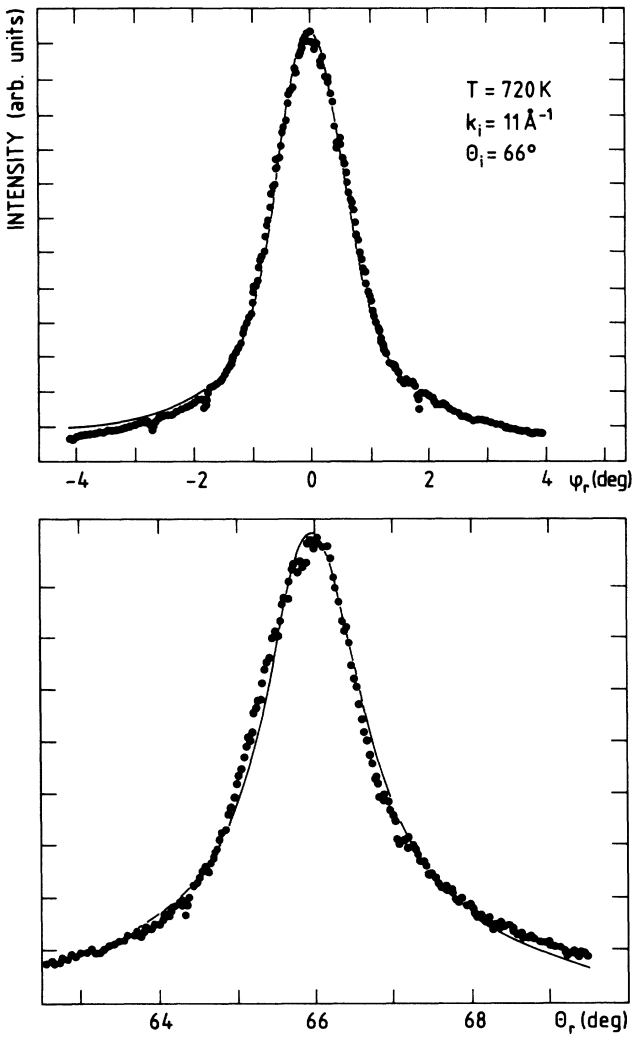

FIG. 8. Cu(113)/He. Typical fit of the scattered intensity (specular peak) in (θ_r) and out (φ_r) of the incidence plane. Incidence was normal to steps.

scattering is not sensitive to phase or antiphase conditions. For the peak profiles in antiphase conditions the change of shape with temperature is apparent in Fig. 7.

The global instrumental function was chosen in order to yield the observed specular shape for in-phase conditions. Figure 8 shows some of the adjustments obtained by this method. Figure 9 shows the exponent $\tau/2$ and the anisotropy η/η' as functions of T. For $T \geq 900$ K no reliable values of the anisotropy could be obtained due to the influence of background on the fitting procedure. Using the analytical expressions for the anisotropic BCSOS model for these two quantities resulted in a very satisfactory fit, with $W_0 = J_y = 800 \pm 50$ K and $W_n = 2J_x = 560 \pm 50$ K, together with $T_R = 720 \pm 50$ K. As has been stated above, the analytical expression for the anisotropy is only an approximate one. However, because it agrees quite well with the MC data for similar models, it may be used to get a direct estimate for the parameters W_0 and W_n. Indeed, as shown in Fig. 9, for these values of W_0 and W_n Monte Carlo data on the DG and TSK models agree nicely with the experimental data. Our value of T_R is not far from that determined by Liang *et al.*,[17] who found $T_R = 620 \pm 10$ K; however, their estimate is clearly out of our error bars. As for W_0 and W_n, we strongly disagree with their results ($W_0 = 2100 \pm 75$ K, $W_n = 86 \pm 10$ K).

For a possible explanation of this disagreement, let us first recall that an analysis of He-diffraction data (intensity-versus-T curves) very similar to Liang's analysis of grazing-x-ray data has been performed by Selke and Szpilka with a VGL-type Hamiltonian. As stated in the Introduction they found $T_R = 650 \pm 50$ K and showed that the decrease in intensity sets in appreciably below the roughening transition temperature (typically at $0.8T_R$). Most importantly, such a behavior was found for various anisotropies (from $W_n/W_0 = 1$ down to 0.014) and therefore it does not depend strongly on the actual value of W_n/W_0. In our opinion this clearly shows that measuring the peak height versus temperature is quite insufficient for an evaluation of W_n and W_0. Peak-shape measurements seem to be crucial for determining W_0 and W_n. In other words, it is necessary to measure the form factor from which correlation func-

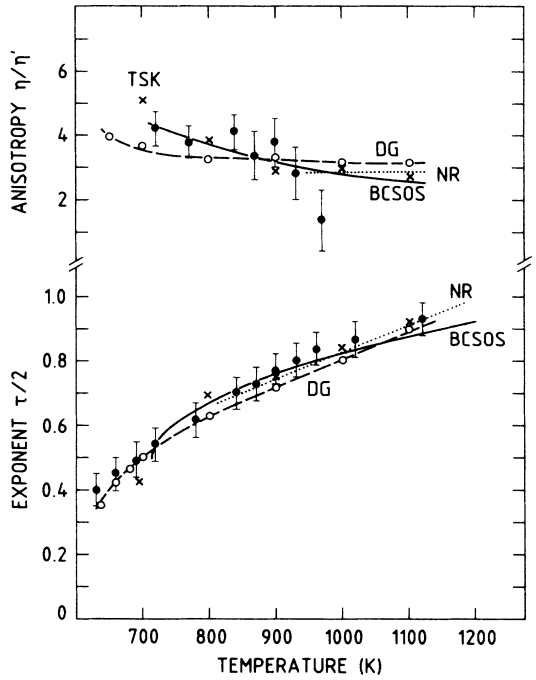

FIG. 9. Adjustment of the experimentally observed values of η/η' and $\tau/2$ (error bars). The solid line corresponds to the anisotropic BCSOS model, ○ to the discrete Gaussian (DG) model; the dotted line shows unrenormalized (NR) results and the dashed line is a guide for the eye for DG results. $J_x = 800$ K, $J_y = 280$ K. × corresponds to the TSK model ($W_0 = 800$ K, $W_n = 560$ K).

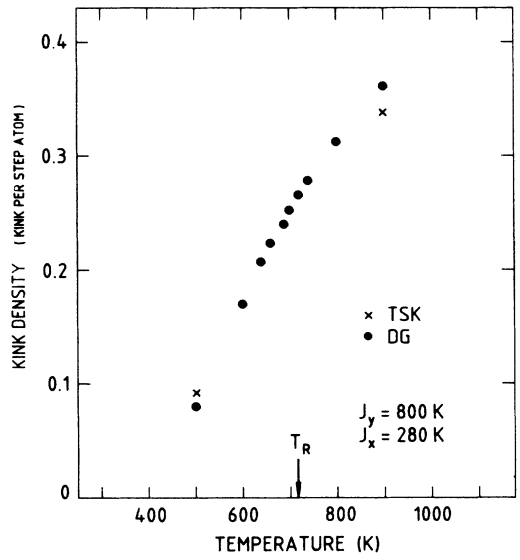

FIG. 10. Kink density along steps calculated in a Monte Carlo simulation of the DG model; a few values for the TSK model are introduced for the sake of verification.

tions can be deduced. It is noticeable that, for He diffraction, spectra can be obtained for temperatures as high as 970 K (see Figs. 7 and 8), whereas the grazing-x-ray measurements of Liang *et al.* only show a structureless background already for $T > 600$ K.

As can be seen in Fig. 9, the predicted cusp of $\tau/2$ near T_R is very small and consequently difficult to observe. One must notice that the peak shape is still a power law for $T \lesssim T_R$, so that values of $\tau/2$ and η/η' are obtained even below the roughening point.

This can be understood if one realizes that the coherence length of our instrument is limited to about 100 Å, so that correlations are only observable up to distances of that order. It is well known from Monte Carlo calculations that an apparent logarithmic behavior is observed below T_R if only short distances are probed.[13] In order to make this statement more quantitative, we carried out MC calculations for the discrete Gaussian model corresponding to $J_y = 800$ K and $J_x = 280$ K. We used the DG model (for which computer programs were less time consuming) and as a criterion for logarithmic behavior we chose to test the correlation function $G(m,0)$ for $1 \leq m \leq 10$, which corresponds to about 50 Å. Using the above criterion, we obtained an apparent logarithmic behavior for temperatures as low as 650 K, i.e., 10% below the roughening transition. So it is clear that the cusp near T_R can be blurred due to limited transfer length as shown here or for even larger samples by Saito *et al.*[18] So it appears such a cusp would only be visible if the transfer length of the apparatus were of the order of a few thousand Å.

From our Monte Carlo calculations the density of kinks could be easily extracted. As shown in Fig. 10, the number of kinks steadily increases with temperature, without obvious singularity in the vicinity of T_R, and reaches 0.25 for $T = 720$ K, corresponding to one kink every fourth step atom on the average.

The value of the kink-creation energy is much lower than what can be deduced from a broken-bond calculation (~ 3000 K; see VGL), but not far from a tight-binding–type calculation [W_0 = (cohesion energy)/32 = 1200 K].[19] More sophisticated calculations would be necessary to understand better the value experimentally determined.

The value of $\eta/\eta' \simeq 4$ is clearly not unity, in contrast to the theory of den Nijs *et al.* Moreover, the ratio of roughening temperatures for Cu(113) and Cu(115) is 720/380 = 1.89, whereas den Nijs *et al.* predict $T_R(113)/T_R(115) = 25/9 = 2.78$. On the other hand, the VGL approach in terms of kink-creation energy and step-step interaction applied through the TSK or similar models explains the present results and allows quantitative estimation of defect-creation energies.

IV. SUMMARY

From the measurements of helium peak shapes on Cu(113) we have deduced both the roughness parameter $\tau/2$ and the anisotropy η/η', thus obtaining a full description of the correlation function. The roughening temperature was found to be $T_R = 720 \pm 50$ K. By using Monte Carlo calculations we were able to fit the experimentally observed thermal behavior of $\tau/2$ and η/η'. We could determine the kink-creation energy $W_0 = 800 \pm 50$ K as well as the energy per atom for shifting a step with respect to the neighboring ones, $W_n = 560 \pm 50$ K

[1]W. K. Burton, N. Cabrera, and F. C. Frank, Philos. Trans. R. Soc. London, Ser. A **243**, 299 (1951).

[2]For reviews, see H. van Beijeren and I. Nolden, in *Structures and Dynamics of Surface II,* edited by W. Schommers and P. Von Blanckenhagen (Springer, Heidelberg, 1987); J. D. Weeks, in *Ordering of Strongly Fluctuating Condensed Matter Systems,* edited by T. Riste (Plenum, New York, 1980).

[3]J. M. Kosterlitz and D. J. Thouless, J. Phys. C **6**, 1181 (1973); J. M. Kosterlitz, *ibid.* **7**, 1046 (1974).

[4]K. O. Keshihev, A. Ya. Parshin, and A. C. Babkin, Z. Eksp. Teor. Fiz. **80**, 716 (1981); J. E. Avov, L. S. Balfour, C. G. Kuper, J. Landau, S. G. Libson, and L. S. Schuman, Phys. Rev. Lett. **45**, 814 (1980); S. Balibar and B. Castaing, J. Phys. Lett. **41**, L329 (1980).

[5]J. Lapujoulade, J. Perreau, and A. Kara, Surf. Sci. **129**, 59 (1983).

[6]J. Villain, D. R. Grempel, and J. Lapujoulade, J. Phys. F **15**, 809 (1985).

[7]M. den Nijs, E. K. Riedel, E. H. Conrad, and T. Engel, Phys. Rev. Lett. **55**, 1689 (1985); **57**, 1279(E) (1986); E. H. Conrad, R. M. Aten, D. S. Kaufman, L. R. Allen, T. Engel, M. den Nijs, and E. K. Riedel, J. Chem. Phys. **84**, 1015 (1986); **85**, 4856(E) (1986).

[8]J. Lapujoulade, Surf. Sci. **178**, 406 (1986); F. Fabre, D. Gorse, J. Lapujoulade, and B. Salanon, Europhys. Lett. **3**, 737 (1987); F. Fabre, D. Gorse, B. Salanon, and J. Lapujoulade, J. Phys. (Paris) **48**, 1017 (1987).

[9]E. H. Conrad, L. R. Allen, D. L. Blachard, and T. Engel, Surf. Sci. **187**, 265 (1987).

[10]W. Selke and A. M. Szpilka, Z. Phys. B **62**, 381 (1986); W. Selke, J. Phys. C **20**, L455 (1987).

[11]H. van Beijeren, Phys. Rev. Lett. **38**, 993 (1977).

[12]R. W. Youngblood, J. D. Axe, and B. M. McCoy, in *Ordering in Strongly Fluctuating Condensed Matter Systems,* edited by T. Riste (Plenum, New York, 1980).

[13]R. W. Youngblood, J. D. Axe, and B. M. McCoy, Phys. Rev. B **21**, 5212 (1980).

[14]S. T. Chui and J. D. Weeks, Phys. Rev. B **14**, 4978 (1976).

[15]W. J. Shugard, J. D. Weeks, and G. H. Gilmer, Phys. Rev. Lett. **41**, 1399 (1978), and references therein.

[16]J. Lapujoulade, Y. Le Cruër, M. Lefort, Y. Lejay, and E. Maurel, Surf. Sci. **118**, L693 (1982).

[17]K. S. Liang, E. B. Sirota, K. L. D'Amico, G. J. Hughes, and S. K. Sinha, Phys. Rev. Lett. **59**, 2447 (1987).

[18]Y. Saito and H. Müller-Krumbhaar, Phys. Rev. B **23**, 308 (1981).

[19]G. Allan and J. Wach, in *Proceedings of the Fourth International Conference on Solid Surfaces, Cannes, 1980,* Le Vide les Couches Minces No. 201 (Flammarion, Paris, 1981).